PRESSURE MEASUREMENTS ABOVE MECHANICALLY GENERATED WATER WAVES (I)

Mizuno, Shinjiro
Research Institute for Applied Mechanics, Kyushu University : Associate Proffessor

https://doi.org/10.5109/6610196

出版情報：Reports of Research Institute for Applied Mechanics. 23 (75), pp.113-129, 1976-02.
九州大学応用力学研究所
バージョン：
権利関係：

Reports of Research Institute for Applied Mechanics
Vol. XXIII, No. 75, 1976

PRESSURE MEASUREMENTS ABOVE MECHANICALLY GENERATED WATER WAVES (I)

By Shinjiro MIZUNO*

Simultaneous measurements of surface pressure and water surface elevation were made under an adverse wind speed of 7.5 m/sec for waves with periods of 0.8, 1.0, 1.2, and 1.6 sec in a wind-wave tunnel, using a servo-mechanical wave following device on which a disk-shaped pressure probe is mounted. Pressure measurements show that wave-induced pressure is much influenced by the disturbances generated at the air outlet which fluctuate with wave period independently of the location. In order to avoid the disturbances due to the air outlet, it is necessary to make simultaneous measurements of pressure and waves over one wave length in the direction of wave propagation, and then it is possible to obtain the net energy flux between the air flow and waves. The experimental results show that the attenuation rates in an adverse wind are of the same order of magnitude as the growth rates obtained by Shemdin in a favorable wind.

1. Introduction

Pressure measurements above mechanically generated waves are conducted under an adverse wind using a wave following device. Shemdin[1] made detailed measurements of surface pressure and air velocity above mechanically generated waves under a favorable wind in a wind-water tunnel, and found the growth rates to be of the same order of magnitude as the theoretical predictions of the Miles[2] invicid theory. As pointed out by Phillips[3], however, when the wind and the waves are in opposition, there is no critical layer where the wind and waves speeds are equal, so that Miles's mechanism for wave generation cannot operate in reverse. It is thus interesting to examine whether or not the wave attenuation in an adverse wind is comparable to the wave growth in a favorable wind.

Field studies of surface pressure on wind-generated waves were made by Dobson[4], Elliott[5], and Snyder[6]. As summarized by Snyder, three independent field experiments yield different growth rates, i.e. the growth rates observed by Snyder, which are comparable with the predictions of the Miles[2] invicid theory,

* Associate Proffessor, Research Institute for Applied Mechanics, Kyushu University, Fukuoka, Japan.

are about one-tenth as large as those observed by Dobson and one-half as large as those obtained by Elliott.

The purpose of the present study is to obtain the energy flux extracted from waves by normal pressure under an adverse wind, and to compare it with the rates of wave attenuation obtained directly from wave height distribution, by means of simultaneous measurements of surface pressure and surface elevation.

2. Experimental apparatus and procedures

Experiments were made in a wind wave tunnel 80 cm high, 60 cm wide and with an effective length of the test section, 850 cm. The depth of air and water was 46 cm and 34 cm respectively. The detailes of the facility were described in a previous paper[7]. Monochromatic waves were generated mechanically, and at the same time a steady adverse wind blew over the water surface. The air leaving the working section of the tunnel was discharged into atmosphere through the outlet just upwind of the wave generator, as shown in Fig. 1.

Simultaneous measurements of waves and pressure were made using a commercially manufactured servo-type wave following device (Keisoku Giken K. K.). A pressure probe, which consisted of a circular disk of 8 mm diameter with a pressure hole of 1 mm at the center, was mounted on the wave following device by spacing at in the spanwise direction 2 cm apart from the sensing element of the device to measure the pressure fluctuations at a fixed height 1.5 cm above the moving water surface. A difference between the pressure above the water surface and the pressure at still atmosphere outside the tunnel was sensed by a commercially manufactured differential pressure transducer with 0.01 kg/cm^2 full scale (Toyo Sokki K. K.).

The length of vinyl tubing connecting the disk-shaped probe to the transducer was changed to make a correction for the pressure phase shift introduced by acoustic delay. The effect of the length of vinyl tubing on the pressure phase shift is considerably remarkable as shown in Fig. 2, so that the tube length must be as short as possible. We used vinyl tubing of 1.0 m in length and made the correction for the phase shift, i.e. 0.5, 1.0, 1.5, and 2.0 degrees for the waves of periods 1.6, 1.2, 1.0 and 0.8 sec, respectively, in the calculation of wave attenuation.

The motion of the wave following device produced the pressure disturbances by tube deformation, which were negligibly small in comparison with wave-induced pressure components for an air speed higher than 2.5 m/sec. For air speed higher than 10.0 m/sec, however, the pressure measurements became impossible because the wave following device could not follow the instantaneous water surface on account of the rapid growth of wind waves. Therefore most of the present experiments were made only for a reference air speed of 7.5 m/sec.

After passing through low pass filters with cutoff frequency $f_c = 11.2$ Hz, wave and pressure signals were digitized with 2 channels A-D converter, and

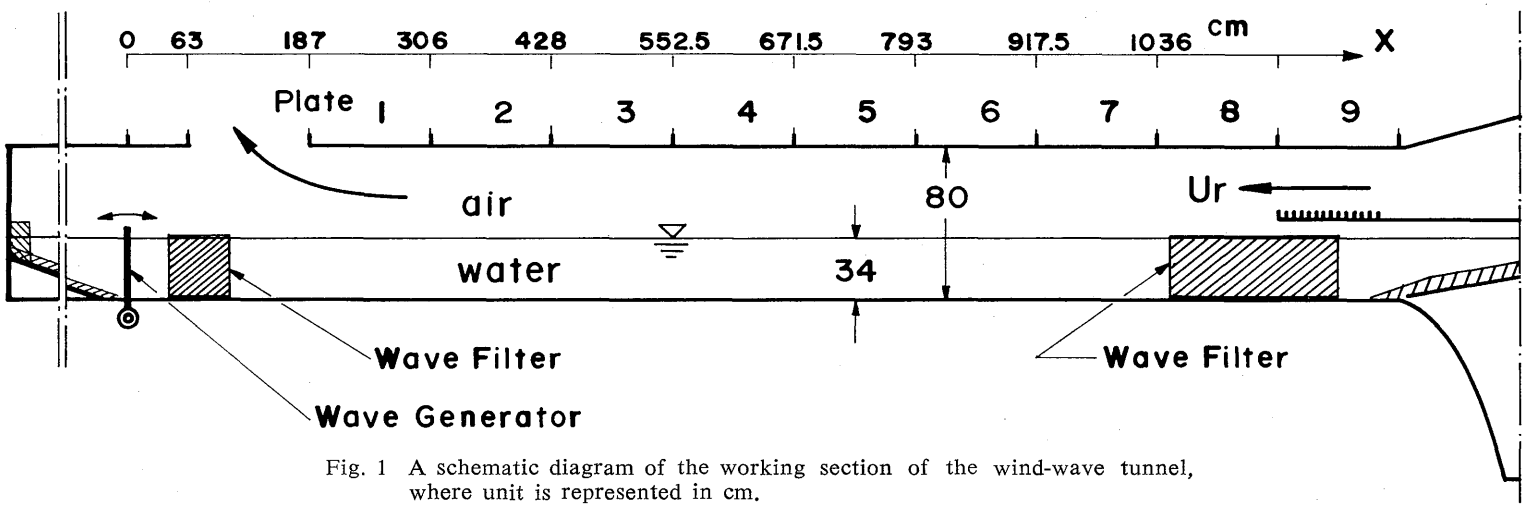

Fig. 1 A schematic diagram of the working section of the wind-wave tunnel, where unit is represented in cm.

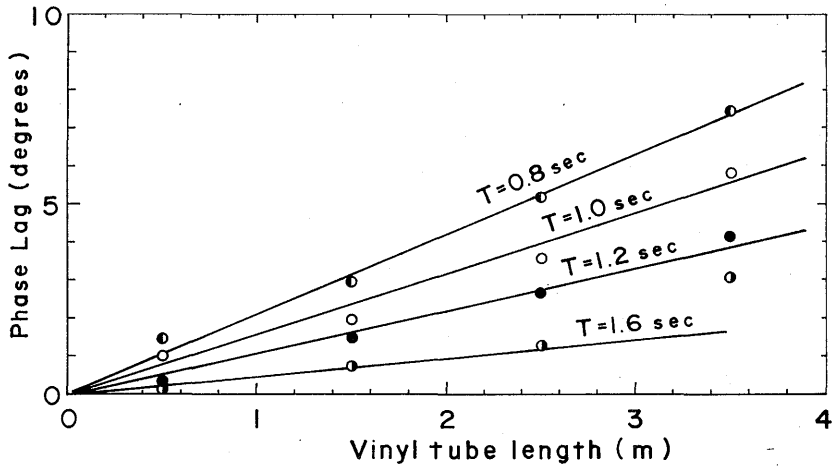

Fig. 2 The acoustic phase lag due to the length of vinyl tubing at $U_r = 7.5$ m/sec.

the calculation of cross-spectral analysis was done immediately using a YHP-2100-A mini-computer, and the power spectra, cross-spectra, coherence, phase and so on were typed out only for the fundamental harmonic of the mechanically generated waves. The flow chart of the experimental procedure is shown in Fig. 3.

3. Experimental results and discussions

3.1 Simultaneous wave and pressure data

When the fundamental harmonic of mechanically generated waves is given by

$$\eta = R_e(\eta_0 e^{i(\omega t - kx)}), \tag{1}$$

the wave-induced pressure at the surface is defined as follows:

$$P = (a+ib)\ \rho_a g\eta \tag{2}$$

where a and b are the normalized in-phase and out-of-phase pressure components, ρ_a is air density, and g is the acceleration of gravity. The above definition is the same as used by Shemdin[2]. The energy flux, F, from wind to waves is directly related to b

$$F = -\overline{P\frac{\partial \eta}{\partial t}} = \rho_a g\omega \left(\frac{\eta_0^2}{2}\right) b, \tag{3}$$

where the over bar indicates time average over many cycles of waves, and since the phase, $\theta(=\tan^{-1}b/a)$, is a key parameter in energy transfer, we first examine how the phase changes with the periods of mechanically generated waves under an adverse wind. Fig. 4 shows a typical result of the phase

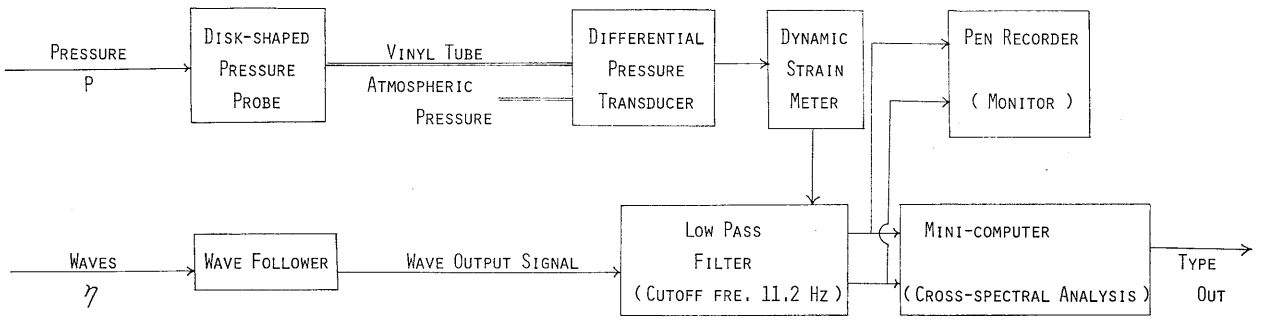

Fig. 3 Block diagram of the experimental apparatus for simultaneous measurements of surface pressure and waves.

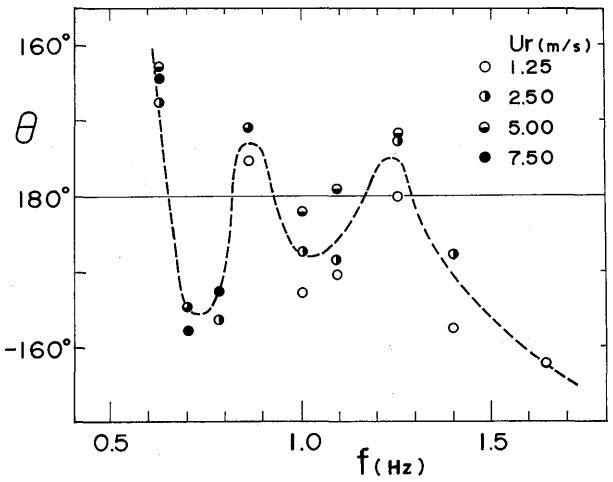

Fig. 4 Phase variation against wave frequencies at a fixed station, $X = 656$ cm.

variation which was measured at station $X=656$ cm from the wave generator as a function of frequencies for several reference air speeds. A striking feature of the phase variation is that the phase is never a slowly changing function of wave frequencies contrary to our expectations, but that it changes rapidly with wave frequencies and takes both positive and negative signs. This means that the direction of energy and momentum transfer from wind to waves alters with wave frequencies. This is contradictory to our previous results that mechanically generated waves attenuated slowly in the direction of wave propagation under an adverse wind[7]. Therefore it is unreasonable to consider that the phase variation such as shown in Fig. 4 has a direct connection with wave growth (or damping).

While trying several experiments to examine its causes, we immediately found the primary cause of the phase variation, that is, an alteration of the air outlet position brought about a marked change of the phase shift. In order to examine how the outlet position are related to the wave-induced pressure on the water surface, detailed distributions of wave height and pressure were measured in the direction of wave propagation for two different outlet positions: one is the usual boundary condition, which was set by removing one of the roof plates of the test section (see Fig. 1), and the other was set by removing furthermore another roof plate (roof plate 1 in Fig. 1). For the wind speed of 7.5 m/sec and wave period of 1.2 sec, the streamwise distributions of wave amplitude H, normalized pressure intensity $P_1/\rho_0 g\eta_0$, and phase shift θ were obtained as a function of a distance from the wave generator, X(Fig. 5-(1)), and as a function of a distance from the downwind end of the working section, X-X^* (Fig. 5-(2)) for the above two outlet boundary conditions, respectively.

Comparison of both figures indicates the following:

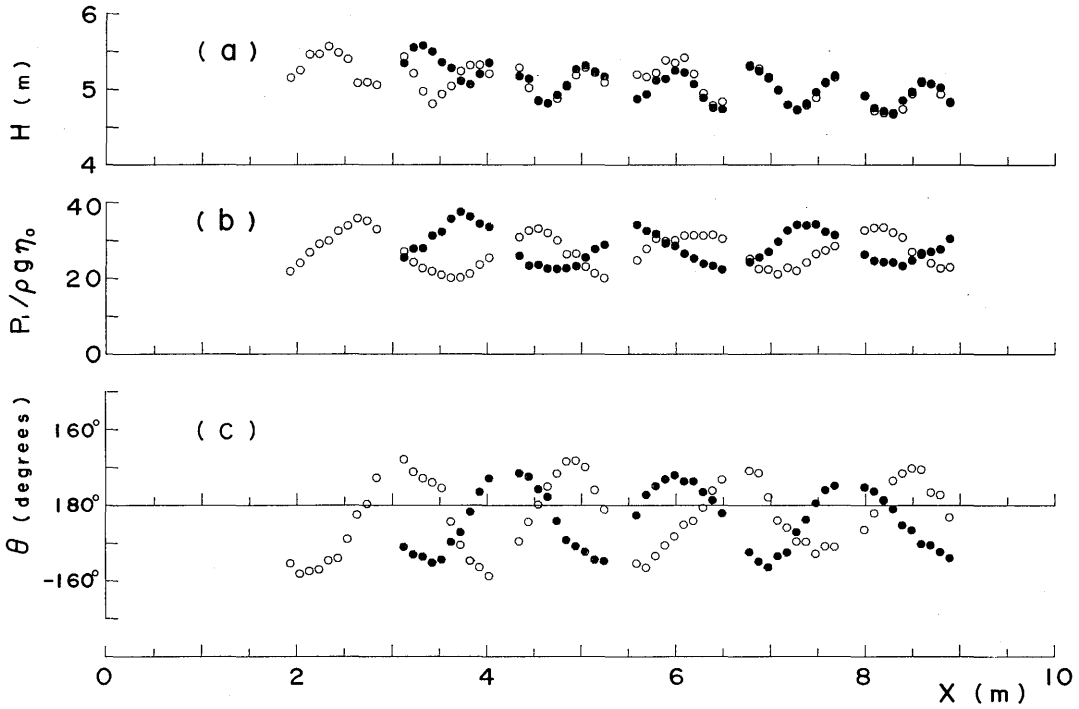

Fig. 5-(1) Streamwise distributions of (a) wave height, (b) normalized pressure intensity at the water surface, and (c) the phase angles between waves and pressure; $U_r = 7.5$ m/sec, $T = 1.2$ sec, where open circles indicate the experimental data for the usual outlet condition, and solid circles those for another outlet condition. X indicates a distance measured from the wave generator.

(1) An alteration of the outlet positions produced very little effect on the distribution of wave height, but had a marked effect on the distribution of pressure intensity and phase.

(2) The wave height varies periodically every half wave length, while the envelope of wave height attenuates gradually in the positive x direction. It is clear that the periodicity of wave amplitude is due to a small amount of a reflection of the mechanically generated waves taking place at the sloping beach.

(3) Both the normalized pressure intensity and phase vary periodically every wave length. Their periodicity can not be explained by the partial reflection of the waves, as will be discussed in detail later.

(4) When they are plotted against the distance from the downwind end of the working section, two sets of streamwise distributions of pressure intensity and phase overlap each other for two different outlet conditions (Fig. 5-(2)).

We assume from the above results that the surface pressure consists of two components:

$$P/\rho_a g a_0 = C_1 \cos(\omega t - kx - \psi) + C_2 \cos \omega t \qquad (4)$$

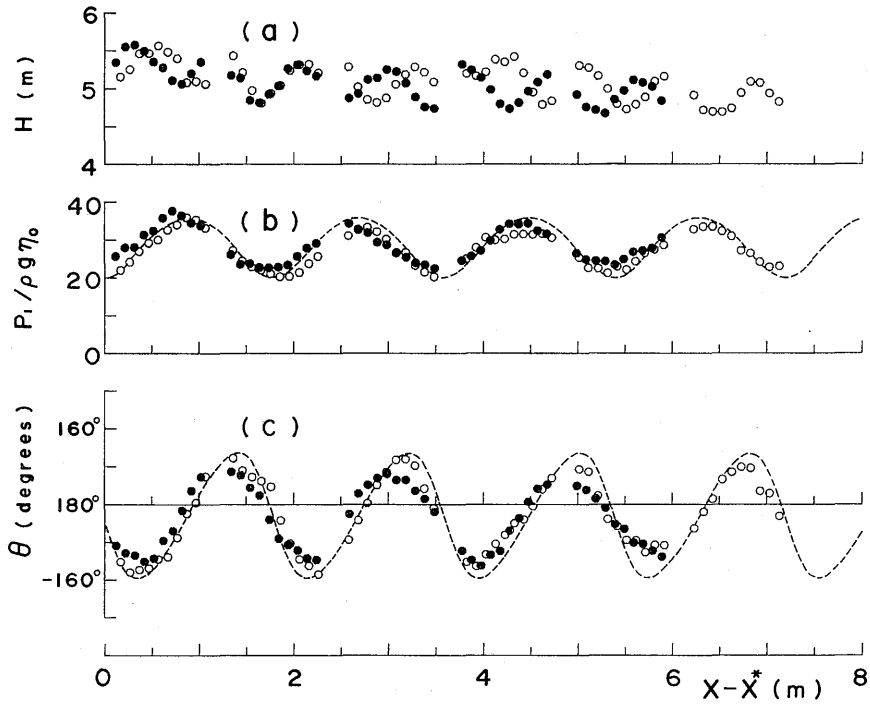

Fig, 5-(2) The experimental data are the same as those of Fig. 5-(1) except that $(X-X^*)$ indicates a distance measured from the downwind end of the working section.

where θ is the phase shift between the surface pressure and surface elevation, the first term of the right hand side indicates the wave-induced pressure component at station x, where x is measured from the downwind end of the working section, and the second term the pressure disturbances which might generate at the outlet, $x=0$. If Eq. (2) is transformed into the following expression

$$P/\rho_a g\eta_0 = C\ \cos\ (\omega t - kx - \theta) \tag{5}$$

then we obtain

$$C = \sqrt{C_1^2 + 2C_1C_2\ \cos\ (kx+\psi) + C_2^2} \tag{6}$$

and

$$\tan\ \theta = \frac{-C_1\ \sin\ kx + C_2\ \sin\ \psi}{C_1\ \cos\ kx + C_2\ \cos\ \psi}. \tag{7}$$

We may roughly estimate the values of the parameter C_1, C_2, and ψ in Eq. (4) from the experimental data (Fig. 5-(2)). The maximum and minimum of C are obtained from Eq. (6) by $C_{\max} = C_1 + C_2$ and $C_{\min} = C_1 - C_2$, where $C_1 > C_2 > 0$ because the first term of Eq. (4) is considered to be greater than the se-

cond. Since $C_{max} = 38$ and $C_{min} = 18$ from the experimental data, we obtain $C_1 = 28$ and $C_2 = 10$. Furthermore, we obtain $\psi = -177°$ from the mean phase of the experimental data. On substituting these values into Eqs. (6) and (7) we can determine the spacial variations of the pressure amplitude C and its phase θ, which are drawn in Fig. 5-(2) by two broken curves. It is seen that both of them agree quite well with the experimental data. Thus we confirm that Eq. (4) is a satisfactory expression for the present pressure data. We also note that for the wave number k, we have taken a somewhat smaller value than the wave number k_0, based on the linear wave theory, to match so well with the experimental data. This is because mechanically generated waves are slightly compressed when propagating against the adverse wind. The compression rate of wave length is approximately 0.03 and agrees well with that obtained by a different method of measurement[7].

We now consider why the second term of Eq. (4) should appear in the present experiments. The air leaving the working section of the tunnel is discharged through the removed roof plate (or plates) into atmosphere without recovering its kinetic energy in the form of pressure energy. The pressure loss at the outlet will depend not only on the air speed but also on the cross-sectional area of the tunnel, which contracts or enlarges with the water surface by the presence of waves. Therefore a possibility is suggested that just at the outlet will the pressure disturbances generate in the form of sound waves whose frequency is the same as that of the mechanically generated waves, and that they will propagate along the tunnel with sound speed. The pressure of infinitesimal sound waves propagating in the positive x direction, of course, is given by

$$P_s = a_0 \cos\ (\omega t - k_s x), \tag{8}$$

where k_s is the wave-number of sound waves.

As compared with the second term in Eq. (4), P_s includes an additional term, $k_s x$, in the argument. It may, however, be neglected in the present experimental conditions because x, a distance from the sound source, is much less than the wave length of sound waves whose frequency is equal to that of mechanically generated waves. Thus the second term in Eq. (4) may be considered to represent a contribution from the sound source at the air outlet. Yet, there is also a possibility of the contribution from the vertical motion of the wave following device, because it is proportional to $\cos \omega t$. Its contribution, however, is negligibly small since the second term in Eq. (4) is about ten times as large as the static pressure term due to the vertical motion of the device for the experimental data of Fig. 5.

On substituting Eq. (4) into Eq. (3), we now obtain

$$F = \rho_a g \omega \left(\frac{\eta_0^2}{2}\right) [C_1 \sin \psi - C_2 \sin kx] \tag{9}$$

If Eq. (9) is averaged over a wave length in the x direction, the second term disappears and does not contribute to the net energy flux, i.e. to the energy

flux directly related to wave growth. Therefore we conclude that in order to obtain the net energy flux, it is necessary to make simultaneous measurements of pressure and waves over more than one wave length in the x direction, and to integrate the product of the out-of-phase components of pressure and the surface elevation over the integral multiple of wave length.

Finally pressure measurements of the present experiments show that since the surface pressure fluctuations above waves are very sensitive to external disturbances propagating from some sources, it is particularly desirable carefully to examine the effects of external disturbances on the wave-induced pressure fluctuations. The same would be also true for atmospheric pressure fluctuations. For example, Snyder[6] suggests from the analysis of directional wave spectra that atmospheric fluctuations above wind waves are often dominated by the up-wind travelling pressure fluctuations, which are primarily due to reflection from a laboratory vessel or shore.

3.2 The rates of wave attenuation

Simultaneous measurements of surface pressure and wave height such as shown in Fig. 5 were also made for wave periods of 0.8, 1.0, and 1.6 sec at the adverse wind speed of 7.5 m/sec. The detailes of the experimental results are summarized in the appendix, together with those of $T = 1.2$ sec. The rates of wave attenuation were calculated using those experimental results obtained by two different methods; one is from the energy flux into waves by normal pressure, and the other is from wave height distribution in the x-direction. The growth rates ξ_p due to the energy flux method are defined by

$$\xi_p = F/\omega E = \frac{\rho_a}{\rho_w} <b> \tag{10}$$

where, E is the wave energy per unit area, ρ_w water density, and $< >$ indicates averaging over one wave length in the x-direction. On the other hand, for a stationary wind and wave system the spatial growth rates ε are obtained from wave height distribution as follows:

$$H = H_0 \exp\left(\varepsilon \frac{x}{L_0}\right) \tag{11}$$

where L_0 indicates the wave length based on the linear wave theory. In a wave tank, however, waves also damp due to viscous friction at the side wall and bottom and by wave motions. Since the wave damping due to friction is given by the growth rate ε_0 obtained when there is no wind blowing over the waves, the net growth rate ε_w becomes $(\varepsilon - \varepsilon_0)$. Then, the growth rates with respect to time, ξ_w, are related to ε_w by

$$\xi_w = \frac{1}{\omega E} \frac{dE}{dt} = \frac{C_g}{\omega E} \frac{\partial E}{\partial x} = \frac{1}{\pi} \frac{C_g}{C_0} \varepsilon_w, \tag{12}$$

where C_g is the group velocity of waves.

The measured data such as the mean wave heights, the net normalized pressure

Table 1 The experimental results of normalized pressure averaged over x, and the growth rates obtained from the energy flux due to surface pressure and from wave height distribution.

CASE No.	T (sec)	H (cm)	H/L_0	$-<a>$	$-<b>$	θ (degree)	$-\xi_p \times 10^3$	$-\varepsilon$	$-\varepsilon_0$	$-\xi_w \times 10^3$	$\xi_p/\xi_w \times 100$ (%)
1	0.8	2.2	0.023	34.5	4.0	−172	4.7	0.08～0.11	0.004	14～19	24～33
2	1.0	6.7	0.047	26.0	3.3	−171	3.0	0.063	0.005	11	28
3	1.2	5.1	0.028	26.8	0.9	−177	1.0	0.025	0.10	3.5	28
4	1.2	5.1	0.028	28.0	0.9	−177	1.0	0.026	0.10	3.7	27
5	1.6	6.3	0.025	20.5	2.1	−174	2.5	0.093	0.12	25	10

components, and the growth rates ξ_p and ξ_w, were calculated, and summarized in Table 1, where the growth rates ξ_w were calculated graphically from the gradient of the envelope of wave heights by plotting the experimental values shown in the appendix on log-linear graph paper. The wave height distribution for the waves of $T = 0.8$ sec does not decrease monotonously, so that the ξ_w was calculated by using only the experimental values within the range of wave height distribution which shows a monotonous decrease.

The rerults shown in Table 1 indicates the following:

(1) The in-phase pressure components $<a>$ are an order of magnitude larger than the out-of-phase one $<b>$, indicating that the phase angles θ are near 180°.

(2) $<b>$ are negative for all the waves measured, indicating wae attention.

(3) The attenuation rates ξ_p are about 30 % of ξ_w, those obtained from wave height distribution, except the waves of $T = 1.6$ sec. We note that the coherence between pressure and waves was very high, i.e. nearly 1, for the fundamental harmonic.

The out-of-phase pressure components $<b>$ of the present data are compared in Fig. 6 with those obtained by Shemdin[1] as a function of C_0/U^* where U^* is friction velocity and approximately 40 cm/sec for the present data[7], and absolute values of $<b>$ are plotted. Although Shemdin made the pressure measurements in the frequency range of 0.4 Hz to 0.78 Hz in a favorable wind for simple waves and non-simple waves which were consisted of two simple waves, only the simple waves of frequencies of 0.6 and 0.78 Hz were selected for the comparison because the measurement conditions are almost the same as the present ones. It is evident that both data agree well with each other, in particular, for the waves of the same frequencies. Accordingly, although the experimental data are very few, we can draw an interesting conclusion that the attenuation rates under an adverse wind are of the same order of magnitude as the growth rates under a favorable wind.

Phillips[3] proposed an attenuation mechanism, which arises from the undulatory flow of the turbulence over the water surface. This mechanism does not seem to operate in the present case because the experimental values are one order of magnitude larger than predicted by the Phillips's theory, and C_0/U_* is

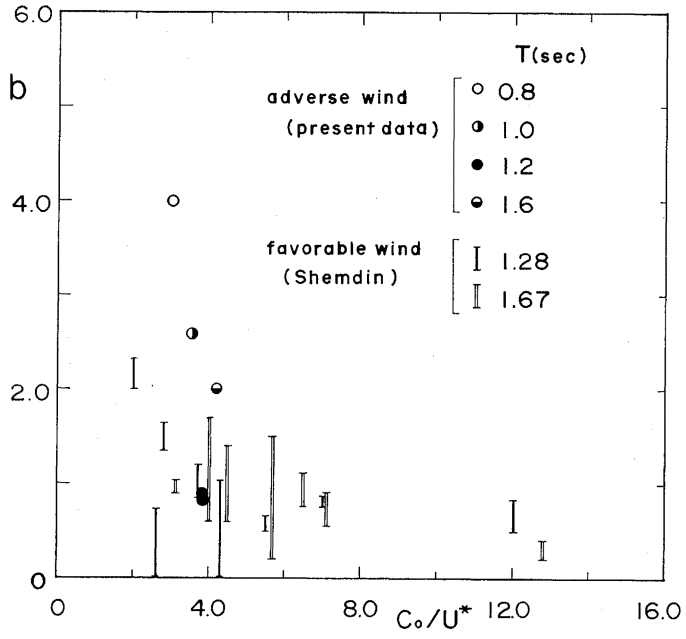

Fig. 6 Comparison between the out-of-phase pressure components in a favorable wind and those in an adverse wind, for which absolute values of $\langle b \rangle$ are plotted.

beyond the limits required by the theory.

4. Conclusions

(1) The wave-induced pressure fluctuations above mechanically generated waves seem to be caused also by the contraction and enlargement of the cross sectional area at the downwind end of the working section produced when mechanically generated waves pass through the air outlet.

(2) On account of the presence of the pressure disturbances the energy flux from waves toward wind at one station obtained from simultaneous measurements of surface pressure and surface displacement of water could not be directly related to the wave attenuation.

(3) The energy flux directly related to the wave attenuation is given by the one averaged over one wave length in the direction of wave propagation.

(4) The attenuation rates obtained from pressure measurements are roughly 30 % of those obtained from wave height distributions.

(5) The attenuation rates estimated from pressure measurements in an adverse wind condition seem to be of the same order of magnitude as the wave growth rates obtained by Shemdin in a favorable wind condition.

Acknowledgements

The author wishes to thank Professor *H.* Mitsuyasu for many valuable discussions and suggestions, and to Mr. A. Masuda for his helpful discussions. He is also indebted to Mr. M. Tanaka for his considerable assistance with the experiments, to Mr. K. Eto for drawing the figures, and to Miss N. Uraguchi for typing the manuscript.

References

1) Shemdin, O. H.: *Instantaneous Velocity And Pressure measurements Above Propagating Waves,* Dept. Coastal and Oceanogr. Eng. Tech. Rep. **4**, University of Florida, Gainesville, (1969).
2) Miles, J. W.: *On the generation of surface waves by shear* flows, *Part 2,* J. Fluid Mech. **6**, (1959). 568-582.
3) Phillips, O. M: *The Dynamics of the Upper Ocean,* (Cambridge University Press, 1966) Chapter, 148.
4) Dobson, F. W.: *Measurements of atmospheric pressure on wind-generated sea waves,* J. Fluid Mech. **48**, (1971) 91-127.
5) Elliott, J. A.: *Microscale pressure fluctuations near waves being generated by the wind,* J. Fluid Mech. **54**, (1972) 427-449.
6) Snyder, R. L.: *A field study of wave-induced pressure fluctuations above surface gravity waves,* J. Mar. Res. **32**, (1974) 497-531.
7) Mizuno, S. and Mitsuyasu, H.: *Effects of Adverse Wind on the Phase Velocity of Mechanically Generated Water Waves,* Rep. Res. Inst. Appl. Mech. Kyushu Univ. **21**, No. 68 (1973) 33-52.

(Received December 8, 1975)

Appendix

Note The experimental values of H, P_2, a, b, phase, and P_1 are given as a function of the distance from the wave generator, X, where PLATE indicates the number of the roof plate in Fig. 1, and P_1 and P_2 were obtained from $P_1=|\overline{\eta P}|/\rho_a g\overline{\eta^2}$ and $P_2=\sqrt{\overline{P^2}}/\rho_a g\sqrt{\overline{\eta^2}}$, respectively. a, b, and phase are not corrected for the acoustic delay due to the length of vinyl tubing. They must be corrected for the vinyl tubing of 1 m length using Fig. 2, when the energy flux is calculated.

CASE NO. 1 T= 0.8SEC U= 7.5M/SEC

PLATE	ORDER	X (CM)	H (CM)	P2	A	B	PHASE (DEGREE)	P1
3	1	435.0	2.30	33.33	-32.90	-4.97	-171.4	33.27
3	2	445.0	2.24	32.28	-31.69	-5.81	-169.6	32.22
3	3	455.0	2.19	34.76	-33.84	-7.45	-167.6	34.65
3	4	465.0	2.24	34.54	-33.88	-6.27	-169.5	34.46
3	5	475.0	2.20	36.10	-35.16	-7.92	-167.3	36.04
3	6	485.0	2.19	37.07	-36.42	-6.73	-169.5	37.03
3	7	495.0	2.14	36.60	-36.17	-5.21	-171.8	36.54
3	8	505.0	2.13	36.42	-36.01	-4.33	-173.2	36.27
3	9	515.0	2.09	36.32	-35.98	-4.58	-172.8	36.27
3	10	525.0	2.12	33.31	-32.81	-5.36	-170.7	33.25
4	1	559.5	2.17	36.41	-35.82	-5.93	-170.6	36.31
4	2	569.5	2.20	36.23	-35.80	-5.07	-171.9	36.15
4	3	579.5	2.20	36.34	-36.05	-3.74	-174.1	36.24
4	4	589.5	2.15	35.39	-35.22	-3.02	-175.1	35.35
4	5	599.5	2.15	35.82	-35.63	-1.91	-176.9	35.68
4	6	609.5	2.09	32.56	-32.27	-3.94	-173.0	32.51
4	7	619.5	2.20	31.49	-31.15	-4.18	-172.4	31.43
4	8	629.5	2.09	31.29	-30.63	-5.94	-169.0	31.20
4	9	639.5	2.08	32.61	-31.63	-7.53	-166.6	32.51
4	10	649.5	2.07	36.38	-35.60	-7.26	-168.5	36.33

CASE NO. 2 T= 1.0SEC U= 7.5M/SEC

PLATE	ORDER	X (CM)	H (CM)	P2	A	B	PHASE (DEGREE)	P1
3	1	435.0	7.36	21.52	-21.43	-1.64	-175.6	21.49
3	2	445.0	7.04	21.59	-21.14	-4.21	-168.7	21.56
3	3	455.0	7.04	23.43	-22.68	-5.82	-165.6	23.42
3	4	465.0	6.93	26.38	-25.16	-7.89	-162.6	26.36
3	5	475.0	6.84	27.77	-26.42	-8.44	-162.3	27.74
3	6	485.0	7.09	29.91	-29.08	-6.95	-166.6	29.90
3	7	495.0	7.01	31.00	-30.22	-6.78	-167.4	30.97
3	8	505.0	7.02	31.34	-30.91	-5.02	-170.8	31.32
3	9	515.0	7.06	32.25	-32.20	-1.52	-177.3	32.23
3	10	525.0	6.78	30.94	-30.93	-0.51	-179.1	30.93
4	1	559.5	6.63	22.46	-22.42	-0.40	-179.0	22.42
4	2	569.5	6.84	21.89	-21.71	-2.56	-173.0	21.86
4	3	579.5	6.77	21.51	-20.92	-4.85	-167.0	21.48
4	4	589.5	6.66	22.90	-21.93	-6.46	-163.6	22.86
4	5	599.5	6.61	25.85	-24.46	-8.28	-161.3	25.82
4	6	609.5	6.47	27.32	-26.04	-8.22	-162.5	27.31
4	7	619.5	6.59	28.94	-28.00	-7.27	-165.5	28.93
4	8	629.5	6.72	31.06	-30.55	-5.47	-169.9	31.04
4	9	639.5	6.64	30.77	-30.51	-3.81	-172.9	30.75
4	10	649.5	6.73	31.06	-30.99	-1.46	-177.3	31.03
5	1	678.5	6.47	27.52	-27.41	2.36	175.1	27.51
5	2	688.5	6.51	25.31	-25.26	1.40	176.8	25.29
5	3	698.5	6.51	23.11	-23.07	0.84	177.9	23.08
5	4	708.5	6.57	21.87	-21.85	-0.61	-178.4	21.86
5	5	718.5	6.47	21.54	-21.28	-3.25	-171.3	21.53
5	6	728.5	6.33	22.22	-21.54	-5.36	-166.0	22.20
5	7	738.5	6.25	23.21	-22.35	-6.21	-164.5	23.20
5	8	748.5	6.28	26.04	-24.86	-7.74	-162.7	26.03
5	9	758.5	6.33	27.97	-26.92	-7.56	-164.3	27.96
5	10	768.5	6.37	28.01	-27.24	-6.45	-166.7	27.99

CASE NO. 3 T= 1.2SEC U= 7.5M/SEC

PLATE	ORDER	X (CM)	H (CM)	P2	A	B	PHASE (DEGREE)	P1
1	1	194.0	5.16	22.10	-21.20	-5.80	-164.7	21.98
1	2	204.0	5.26	24.22	-22.96	-7.49	-161.9	24.15
1	3	214.0	5.47	27.04	-25.70	-8.05	-162.6	26.94
1	4	224.0	5.47	29.27	-27.90	-8.56	-163.0	29.19
1	5	234.0	5.57	30.16	-29.05	-7.57	-165.4	30.02
1	6	244.0	5.49	32.68	-31.65	-7.89	-166.0	32.62
1	7	254.0	5.40	34.09	-33.59	-5.24	-171.1	34.00
1	8	264.0	5.09	35.96	-35.86	-1.58	-177.5	35.89
1	9	274.0	5.10	35.36	-35.30	0.28	179.6	35.30
1	10	284.0	5.06	33.15	-32.82	4.24	172.6	33.09
2	1	313.0	5.44	27.28	-26.56	5.76	167.8	27.18
2	2	323.0	5.22	24.45	-24.10	3.79	171.1	24.40
2	3	333.0	4.98	22.86	-22.62	2.87	172.8	22.80
2	4	343.0	4.81	22.10	-21.87	2.36	173.9	21.99
2	5	353.0	4.94	21.22	-20.93	1.70	175.3	21.00
2	6	363.0	5.05	20.38	-20.17	-1.50	-175.7	20.23
2	7	373.0	5.24	20.42	-19.96	-3.70	-169.5	20.30
2	8	383.0	5.32	21.37	-20.62	-5.41	-165.3	21.32
2	9	393.0	5.33	23.72	-22.70	-6.69	-163.6	23.66
2	10	403.0	5.21	25.67	-24.21	-8.19	-161.3	25.56
3	1	435.0	5.29	31.03	-30.57	-5.11	-170.5	30.99
3	2	445.0	5.03	32.76	-32.61	-2.47	-175.7	32.70
3	3	455.0	4.86	33.30	-33.24	0.17	179.7	33.24
3	4	465.0	4.82	32.18	-31.95	2.87	174.9	32.08
3	5	475.0	4.88	30.15	-29.77	4.44	171.5	30.10
3	6	485.0	5.06	26.51	-25.92	5.37	168.3	26.47
3	7	495.0	5.19	26.71	-26.04	5.48	168.1	26.61
3	8	505.0	5.29	23.27	-22.81	4.44	169.8	23.18
3	9	515.0	5.22	21.51	-21.37	1.55	175.9	21.43
3	10	525.0	5.09	20.24	-20.17	-0.40	-178.9	20.18
4	1	559.5	5.20	24.95	-24.01	-6.62	-164.6	24.91
4	2	569.5	5.17	28.00	-26.78	-7.95	-163.5	27.94
4	3	579.5	5.22	30.73	-29.78	-7.12	-166.6	30.62
4	4	589.5	5.39	30.04	-29.45	-5.52	-169.4	29.97
4	5	599.5	5.35	30.25	-29.90	-4.30	-171.8	30.20
4	6	609.5	5.42	31.45	-31.30	-2.82	-174.9	31.43
4	7	619.5	5.21	31.55	-31.42	-2.27	-175.9	31.50
4	8	629.5	4.95	31.49	-31.41	-0.35	-179.4	31.41
4	9	639.5	4.79	31.65	-31.54	2.19	176.0	31.61
4	10	649.5	4.84	30.62	-30.35	3.67	173.1	30.57
5	1	678.5	5.31	25.37	-24.98	4.06	170.8	25.31
5	2	688.5	5.28	22.70	-22.38	3.37	171.4	22.64
5	3	698.5	5.17	22.58	-22.49	0.89	177.7	22.50
5	4	708.5	5.00	21.28	-21.19	-1.49	-176.0	21.25
5	5	718.5	4.80	23.00	-22.82	-2.35	-174.1	22.94
5	6	728.5	4.73	22.18	-21.81	-3.70	-170.4	22.12
5	7	738.5	4.79	24.42	-23.96	-4.09	-170.3	24.30
5	8	748.5	4.89	26.67	-25.88	-5.94	-167.1	26.55
5	9	758.5	5.10	27.52	-26.97	-5.20	-169.1	27.47
5	10	768.5	5.16	28.64	-28.07	-5.47	-169.0	28.60
6	1	800.0	4.92	32.83	-32.59	-3.69	-173.5	32.80
6	2	810.0	4.72	33.54	-33.46	-1.18	-177.9	33.48
6	3	820.0	4.70	33.62	-33.55	0.84	178.6	33.56
6	4	830.0	4.69	32.29	-32.03	3.68	173.4	32.25
6	5	840.0	4.74	31.08	-30.61	4.56	171.5	30.95
6	6	850.0	4.95	27.16	-26.70	4.63	170.2	27.10
6	7	860.0	5.09	26.49	-26.05	4.37	170.5	26.41
6	8	870.0	5.08	24.24	-24.10	1.47	176.5	24.14
6	9	880.0	4.94	22.87	-22.75	1.14	177.1	22.78
6	10	890.0	4.83	23.16	-23.02	-1.27	-176.8	23.06

CASE NO. 4 T= 1.2SEC U= 7.5M/SEC

PLATE	ORDER	X (CM)	H (CM)	P2	A	B	PHASE (DEGREE)	P1
2	1	313.0	5.35	25.71	-25.17	-4.89	-169.0	25.64
2	2	323.0	5.56	28.01	-27.22	-6.27	-167.0	27.93
2	3	333.0	5.58	28.21	-27.28	-6.59	-166.4	28.07
2	4	343.0	5.50	31.52	-30.30	-8.21	-164.8	31.39
2	5	353.0	5.36	32.48	-31.37	-8.05	-165.6	32.39
2	6	363.0	5.29	35.84	-35.28	-6.01	-170.3	35.79
2	7	373.0	5.12	37.67	-37.31	-4.66	-172.9	37.60
2	8	383.0	5.07	36.48	-36.37	-1.08	-178.3	36.38
2	9	393.0	5.21	34.49	-34.38	2.17	176.4	34.45
2	10	403.0	5.36	33.77	-33.44	4.24	172.8	33.70
3	1	435.0	5.18	26.09	-25.74	3.89	171.4	26.03
3	2	445.0	5.15	23.57	-23.27	3.15	172.3	23.48
3	3	455.0	4.85	23.70	-23.59	1.83	175.6	23.66
3	4	465.0	4.82	22.79	-22.67	0.96	177.6	22.69
3	5	475.0	4.93	22.67	-22.54	-1.62	-175.9	22.60
3	6	485.0	5.04	22.87	-22.49	-3.63	-170.8	22.78
3	7	495.0	5.27	23.40	-22.91	-4.38	-169.2	23.32
3	8	505.0	5.32	25.68	-25.02	-5.46	-167.7	25.61
3	9	515.0	5.24	27.90	-26.97	-6.92	-165.6	27.85
3	10	525.0	5.17	29.11	-28.08	-7.43	-165.2	29.05
4	1	559.5	4.88	34.32	-34.25	-1.57	-177.4	34.28
4	2	569.5	4.94	32.73	-32.64	1.65	177.1	32.68
4	3	579.5	5.12	31.94	-31.76	2.88	174.8	31.89
4	4	589.5	5.14	29.40	-29.12	3.56	173.0	29.33
4	5	599.5	5.25	28.70	-28.38	4.02	171.9	28.67
4	6	609.5	5.23	26.68	-26.46	2.99	173.6	26.63
4	7	619.5	5.07	25.39	-25.20	2.84	173.6	25.36
4	8	629.5	4.89	24.03	-23.91	1.52	176.4	23.96
4	9	639.5	4.76	23.53	-23.42	0.62	178.5	23.42
4	10	649.5	4.74	22.51	-22.45	-0.81	-177.9	22.47
5	1	678.5	5.32	24.48	-23.87	-5.24	-167.6	24.44
5	2	688.5	5.25	25.83	-24.84	-6.60	-165.1	25.70
5	3	698.5	5.15	27.22	-26.07	-7.67	-163.6	27.17
5	4	708.5	4.99	29.90	-29.00	-6.98	-166.5	29.83
5	5	718.5	4.80	32.85	-32.00	-7.08	-167.5	32.77
5	6	728.5	4.74	34.33	-33.98	-4.22	-172.9	34.24
5	7	738.5	4.82	34.13	-34.02	-2.24	-176.2	34.10
5	8	748.5	4.97	34.43	-34.36	0.38	179.4	34.36
5	9	758.5	5.09	32.47	-32.34	2.30	175.9	32.43
5	10	768.5	5.19	31.60	-31.43	2.86	174.8	31.56
6	1	800.0	4.93	26.49	-26.33	2.24	175.1	26.43
6	2	810.0	4.76	24.84	-24.72	1.65	176.2	24.78
6	3	820.0	4.72	24.50	-24.46	0.66	178.5	24.46
6	4	830.0	4.68	24.39	-24.34	-0.40	-179.0	24.34
6	5	840.0	4.86	23.44	-23.28	-2.18	-174.7	23.38
6	6	850.0	4.97	24.94	-24.70	-2.84	-173.4	24.86
6	7	860.0	5.11	26.86	-26.36	-4.80	-169.7	26.79
6	8	870.0	5.08	27.21	-26.68	-4.98	-169.4	27.15
6	9	880.0	5.03	27.86	-27.18	-5.97	-167.6	27.82
6	10	890.0	4.84	30.65	-29.68	-7.43	-166.0	30.59

CASE NO. 5 T= 1.6SEC U= 7.5M/SEC

PLATE	ORDER	X (CM)	H (CM)	P2	A	B	PHASE (DEGREE)	P1
3	1	435.0	6.81	12.48	-12.45	-0.03	-179.8	12.45
3	2	445.0	6.50	12.35	-12.15	-1.86	-171.3	12.29
3	3	455.0	6.44	12.80	-12.36	-3.25	-165.3	12.78
3	4	465.0	6.58	14.08	-13.33	-4.48	-161.4	14.06
3	5	475.0	6.66	16.09	-14.78	-6.33	-156.8	16.08
3	6	485.0	6.82	17.06	-15.38	-7.30	-154.6	17.02
3	7	495.0	6.93	18.12	-16.39	-7.69	-154.9	18.10
3	8	505.0	6.93	20.06	-17.82	-9.16	-152.8	20.03
3	9	515.0	6.87	21.50	-19.35	-9.33	-154.3	21.48
3	10	525.0	6.75	23.05	-20.81	-9.87	-154.6	23.04
4	1	559.5	6.06	28.44	-27.19	-8.26	-163.1	28.42
4	2	569.5	6.00	29.10	-28.35	-6.45	-167.2	29.08
4	3	579.5	6.00	29.75	-29.43	-4.20	-171.9	29.74
4	4	589.5	6.03	29.57	-29.48	-2.12	-175.9	29.55
4	5	599.5	6.18	29.15	-29.14	-0.03	-179.9	29.14
4	6	609.5	6.30	28.07	-27.98	2.15	175.6	28.07
4	7	619.5	6.46	26.72	-26.54	2.96	173.6	26.71
4	8	629.5	6.54	26.12	-25.84	3.64	172.0	26.10
4	9	639.5	6.53	24.64	-24.24	4.39	169.7	24.63
4	10	649.5	6.51	23.54	-22.99	4.99	167.7	23.52
5	1	678.5	6.11	19.45	-18.90	4.55	166.5	19.44
5	2	688.5	5.94	17.74	-17.18	4.37	165.7	17.73
5	3	698.5	5.82	16.46	-16.01	3.64	167.2	16.42
5	4	708.5	5.85	15.04	-14.85	2.34	171.0	15.03
5	5	718.5	5.76	13.88	-13.81	1.25	174.8	13.86
5	6	728.5	5.92	13.13	-13.10	-0.45	-178.0	13.12
5	7	738.5	6.05	13.28	-13.13	-1.84	-172.0	13.26
5	8	748.5	6.16	14.16	-13.64	-3.75	-164.6	14.15
5	9	758.5	6.32	14.73	-14.05	-4.38	-162.7	14.71
5	10	768.5	6.37	16.31	-15.07	-6.21	-157.6	16.30